Ⅲ-4

Surface, Interface and Thin Films

Highlight

BL6U

Bulk and Surface Band Dispersion Mapping of the Au(111) Surface by Newly-developed Acceptance-cone Tunable PES System

F. Matsui[1], H. Yamane[2], T. Ueba[1], T. Horigome[1], S. Makita[1], K. Tanaka[1,3], S. Kera[1,3] and N. Kosugi[3,4]

[1]*UVSOR Synchrotron Facility, Institute for Molecular Science, Okazaki 444-8585, Japan*
[2]*RIKEN SPring-8 Center, Sayo 679-5148, Japan*
[3]*The Graduate University for Advanced Studies (SOKENDAI), Okazaki 444-8585, Japan*
[4]*Institute of Materials Structure Science, KEK, Tsukuba 305-0801, Japan*

Two-dimensional angle-resolved photoelectron (PE) spectroscopy is a powerful method to study the electronic structure of crystal surfaces. The initial state binding energy (E) and the wave vector (**k**) can be determined from the kinetic energy and the direction of the detected PE. The latest version of ARPES analyzer was installed (MB Scientific AB, A-1 analyzer Lens#5) at BL6U (in-house beamline). This PE spectrometer consists of a hemispherical electron analyzer with a mechanical deflector and a mesh electrostatic lens near the sample to make the acceptance cone tunable. A constant energy PE angular distribution of the valence band dispersion cross section in the large **k** range can be efficiently obtained by applying a negative bias voltage to the sample and using the mechanical deflector. Details of the specifications will be reported elsewhere [1].

Here, we introduce three-dimensional band dispersion mapping of the Au single crystal to show the performance of the current PE spectroscopy end station. The Au(111) surface was cleaned by repeating the cycle of Ar+ sputtering and annealing. The cleanliness of the reconstructed Au surface was confirmed by LEED and XPS. ARPES measurement was made at approximately 20 K. The incident photon axis, the electric vector, the normal direction and $\overline{\Gamma M}$ direction of the sample surface and the analyzer entrance slit were all in the horizontal plane. The incident photon axis was offset 60 ° from the surface normal direction.

Figure 1 shows the bias-voltage-dependent band dispersion map in the $\overline{\Gamma M}$ plane. The photon energy was 90 eV. A well-known Au surface state across the Fermi level is observed at $\overline{\Gamma}$ point. The acceptance angle was ±16 °, which corresponding to ±1.2 Å^{-1}. The detection range was expanded to ±3.0 Å^{-1} by applying a negative bias to the sample.

Figure 2 shows the photon-energy-dependent Fermi surface maps with simulated cross sections of bulk Fermi surface. Photon energies of 60, 90, and 120 eV were used for excitation. The bias voltage applied to the sample was fixed to -400 V. The Au(111) surface state at the $\overline{\Gamma}$ point was observed at the center. The hexagonal cross section of the bulk Fermi surface was observed in the angular distribution excited with photon energies of 90 and 120 eV. Note that the observed patterns are more six-fold symmetric, although a three-fold symmetric feature is expected for the second adjacent Brillouin zone. This is probably due to the PE scattering at the surface reconstructed structure. One can not notice such a phenomenon just by measuring the band dispersion at a high symmetry plane.

We greatly acknowledge Dr. P. Baltzer and Ms. M. Matsuki (MB Scientific AB) for their contribution in the construction of the BL6U PE end station.

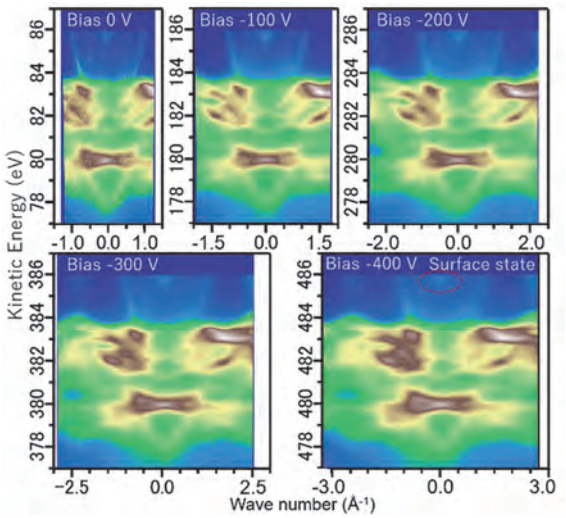

Fig. 1. Band dispersion of the Au(111) surface along $\overline{\Gamma M}$ direction. Photon energy was 90 eV. Various negative bias was applied to the sample.

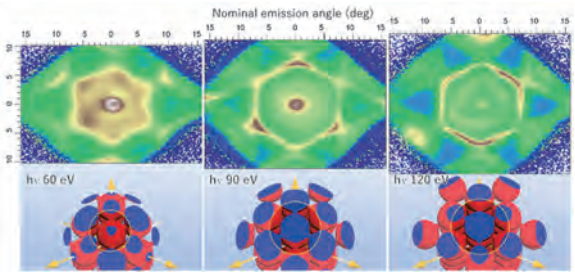

Fig. 2. Fermi surface of the Au(111) surface. Photon energy was varied from 60 eV to 120 eV. Bias voltage of -400 V was applied to the sample.

[1] H. Yamane, F. Matsui, T. Ueba, T. Horigome, S. Makita, K. Tanaka, S. Kera and N. Kosugi, Rev. Sci. Instrum. in Press (2019).

BL2A

Kinetics Investigation to Form Magnesium Hydroxide from Low Crystalline Magnesium Oxide in the Solution

T. Kato[1], K. Takahashi[1], Y. Sawamura[1], M. Kadokura[2] and C. Tokoro[3]
[1]*Graduate School of Creative Science and Engineering, Waseda University, Tokyo 169-8555, Japan*
[2]*School of Creative Science and Engineering, Waseda University, Tokyo 169-8555, Japan*
[3]*Faculty of Science and Engineering, Waseda University, Tokyo 169-8555, Japan*

The low crystalline magnesium oxide, which is produced by heating at 600 degree in 1 hour, has the capacity to remove toxic elements, such as the boron (B), fluorine (F) and so on [1]. In the solution, a part of low crystalline magnesium oxide forms to magnesium hydroxide by the reaction described in equations (1) and (2).

$$MgO\ (s) + H_2O \rightleftarrows Mg^{2+} + 2OH^- \quad (1)$$
$$Mg^{2+} + 2OH^- \rightleftarrows Mg(OH)_2 \quad (2)$$

When a part of low crystalline magnesium oxide precipitates as magnesium hydroxide in the solution, it is suggested that the toxic elements, such as B, F and so on, remove by co-precipitation with magnesium hydroxide. However, the ratio of magnesium hydroxide in the low crystalline magnesium oxide after experiments is not clarified because the structure of precipitation is amorphous. To achieve the quantitative modeling for toxic elements removal by low crystalline magnesium oxide, it is desired that the ratio of magnesium hydroxide in the low crystalline magnesium oxide after experiments evaluates. Thus, the objective of this study is to evaluate the ratio of magnesium hydroxide in the low crystalline magnesium oxide after experiments using x-ray absorption fine structure (XAFS) analysis in magnesium K-edge.

The precipitation after experiments, which the low crystalline magnesium oxide reacted in the solution after 0, 1, 5, 10, 20 and 120 min, was analyzed by XAFS analysis in magnesium K-edge by fluorescence method (Fig. 1). The XAFS spectra of magnesium oxide in magnesium K-edge has two peaks while that of magnesium hydroxide has three peaks in the range of 1300 – 1320 eV [2]. Thus, the x-ray absorption near edge structure (XANES) analysis was performed in the range of 1300 – 1320 eV to evaluate the ratio of magnesium hydroxide in the low crystalline magnesium oxide (Table 1). From XANES results, it was confirmed that almost low crystalline magnesium oxide was precipitated as magnesium hydroxide after 20 min. Using above results, we can construct the quantitative model for toxic elements by low crystalline magnesium oxide.

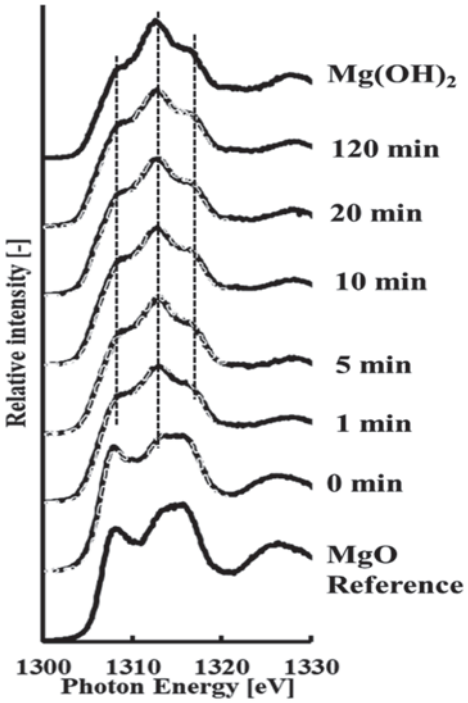

Fig. 1. Magnesium K-edge x-ray absorption fine structure spectra corresponding to x-ray absorption near edge structure region of 0, 1, 5, 10, 20 and 120 min samples, showing resolved components of magnesium oxide and hydroxide based on magnesium oxide and hydroxide reference spectra, respectively.

Table 1. Concentration of magnesium oxide and hydroxide in 0, 1, 5, 10, 20 and 120 min samples, based on x-ray absorption near edge structure analysis in magnesium K-edge [%]

Reaction time [min]	Concentration of MgO	Concentration of $Mg(OH)_2$
0	100	0
1	29.1	70.9
5	16.4	83.6
10	10.1	89.9
20	6.2	93.8
120	0	100

[1] H. Fukuda, S. Hobo, G. Granata, C. Tokoro, Y. Toba and M. Eguchi, Proceedings of the Conference of Metallurgists (2017) 9408.
[2] T. Yoshida, T. Tanaka, H. Yoshida, T. Funabiki and S, Yoshida, J. Phys. Chem. **100** (1996) 2302.

BL2B

Molecular Orientation of DNTT Thin Film on TES-derivatives Deposited Au Substrate

K. K. Okudaira and A. Murafuji
Association of Graduate Schools of Science and Technology, Chiba Univererity, Chiba 263-8522, Japan

Organic devices such as organic light-emitting diodes, organic thin-film transistors (OTFTs), and organic photovoltaic cells, have been attracting interest concerning both fundamental research and practical application for low-cost, large-area, lightweight and flexible devices Recently, OTFT's with field-effect mobility and on/off current ratio comparable to hydrogenated amorphous silicon thin-film transistors.

Since source and drain contact resistance has been identified as a major limitation in OTFTs, control of this interface is important. Several surface treatments have been reported to improve charge injection from metal electrodes into organic semiconductors. A single molecular layer, for example self-assembled monolayer (SAM), has been purposely introduced on top of the electrode as well as insulator surfaces [1]. SAM spontaneously forms by dipping the substrate in a solution of an appropriate reactive surfactant. For the case of application of SAM to the bottom -contact OTFT, where the substrates consist of not only electrodes such as Au but also insulator, it is necessary to use of two types of SAMs for the suitable surfaces of substrates. 6-(3-(triethoxysilyl) propylamino)-1,3,5-triazine-2,4-dithiol monosodium (TES) derivatives have been reported as molecular adhesion, which are able to form the chemical bonds with both insulator such as plastic and metal. TES can be considered as a kind of SAM, which is available to form the chemical bonding (anchoring) to two different substrates.

The characteristics of OTFT such as mobility are considered to be dependence on not only the electronic structure but also the molecular orientation of organic molecule.

In this work we deposited a TES derivative on Au and examined the molecular orientation of dinaphtho[2,3-b:2',3'-f]thieno[3,2-b]thiophene (DNTT) thin films thermally deposited on the TES-derivate surface by angle-resolved ultraviolet photoelectron spectroscopy (ARUPS) measurements. In the ARUPS take-off angle dependence of HOMO peak for π-conjugated organic molecule provides an important information on the molecular orientation [2].

ARUPS measurements were performed at the beam line BL2B of UVSOR III at the Institute for Molecular Science. The take-off angle (β) dependencies of photoelectron spectra were measured with the photon energy (hν) of 28 eV. The Au coated substrate was prepared by depositing Au thin films on natural-oxide Si(001) wafer. We used TES derivatives as coupling agent. The TES layer on Au substrates was prepared using a dipping method at room temperatures. DNTT thin film was deposited on TES.

We observed take-off angle (β) dependence of HOMO peak in UPS of DNTT thin film (thickness of about 6.0 nm on TES-derivates prepared on Au substrate (Fig.1). The peaks originated from π-orbitals including HOMO do not show take-off angle dependence. On the contrary, the intensities of photoelectrons from the σ-states become large as increase take-off angle. For the case of flat-lying molecular orientation of π-conjugated aromatic molecules such as phthalocyanine, the π-peaks show strong take-off angle dependence [3]. It indicates that DNTT molecules have the orientation (not parallel orientation) on TES-derivates Au substrate.

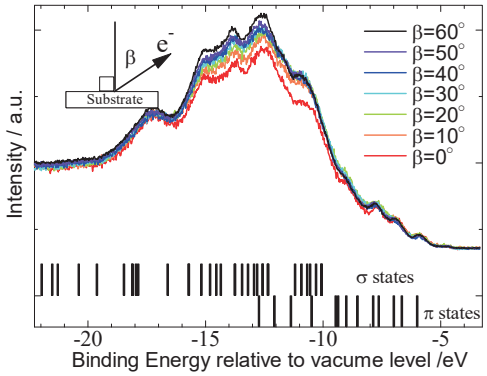

Fig.1. Take-off angle (β) dependences of ultraviolet photoelectron spectra DNTT (6.0nm)/TES/Au.

[1] P. Marmont *et al*., Org Electron. **9** (2008) 419, Y. Horii *et al*., Thin Solid Films **518** (2009) 642.
[2] K. Mori and K. Abe, Hyomen Gijutsu **59** (2008) 299, K. Mori *et al*., J. Soc. Rubber Sci. Technol. **83** (2010) 71.
[3] N. Ueno *et al*., J. Chem. Phys. **99** (1993) 7169.

BL2B

Electronic Structure of Disordered Molecular Heterointerfaces

K. Akaike [1], A. Onishi[1], Y. Wakayama[2] and K. Kanai[1]

[1]*Department of Physics, Faculty of Science and Technology, Tokyo University of Science, Noda 278-8510, Japan*

[2]*International Center for Materials Nanoarchitectonics (WPI-MANA), National Institute for Materials Science (NIMS), Tsukuba 305-0044, Japan*

Intended design of organic heterointerfaces is crucial to control functionality in organic devices based on multi-stacked organic layers. Formation of the heterointerfaces via either vacuum deposition or solution process leads to a variety of interfacial structure; molecular exchange, molecular reorientation, and mixed heteromolecular arrangement. The formation of a well-defined heterointerface is a typically expected consequence, but it is not a sole case. The complicated molecular rearrangement that have been found should introduce structure disorder into the system, but its molecular origin is elusive.

Previously, using scanning tunneling microscopy (STM), we directly observed the disorder formed upon the formation of sexithiophene (6T)/perfluorinated copper phthalocyanine (F_{16}CuPc) interface on a cleaned Ag(111) surface [1]. Deposition of 6T onto an epitaxially grown F_{16}CuPc monolayer perturbed the arrangement of F_{16}CuPc along [1–2] direction. The adsorbed 6T molecules adapted various bent shapes and were randomly mixed with F_{16}CuPc molecules. The bent molecules are originated from *cis-trans* isomerization, in which neighboring thiophene rings rotate. The various molecular shapes of 6T significantly reduced short- and long-range orders.

The STM results prompted us to characterize the electronic structure of such a disordered heterointerfaces, because the Gaussian broadening and tailing of the frontier orbitals are often correlated with structural disorder [2]. In this research, we performed ultraviolet photoelectron spectroscopy (UPS) in BL2B to investigate the energy distribution of the occupied states of 6T/F_{16}CuPc interface.

Figure 1 shows the evolution of the UPS spectra for the interface as a function of 6T coverage in secondary electron cutoff (a) and valence band regions (b). Photon energy of 28 eV was used to acquire the spectra at room temperature. Photoelectron emission angle was fixed to be 45º. The formation of F_{16}CuPc monolayer on Ag(111) reduced work function (WF) by 0.5 eV. This originates from the push-back effect. The highest occupied molecular orbital (HOMO) peak appeared at the binding energy of ~2.1 eV. At the same time, a broad feature was observed just below the Fermi level. The electronic states should be originated from partial occupation of the lowest unoccupied molecular orbital (LUMO) of F_{16}CuPc upon the adsorption on the silver surface.

Increasing coverage of 6T lowered WF by less than 0.1 eV. The WF reduction accompanies with the shift of the F_{16}CuPc HOMO toward lower binding energy. The analysis of the STM images suggested that the nominal coverage of the organic layer reduced upon the deposition of 6T. Therefore, because the bare silver surface has a larger WF, the WF increased upon the interface formation. Unexpectedly, the shape of the HOMO was not broadened by the structural disordering.

Comparable UPS measurements were also carried out for 6T/CuPc/Ag(111) interface. The interface states, formed upon the adsorption of CuPc on the silver surface, shifted toward higher binding energy with increasing 6T coverage. STM images of 6T/CuPc interface suggested the formation of phase-separated binary structure. However, further investigation is necessary to elucidate what molecular arrangement led to the shift of the interface states.

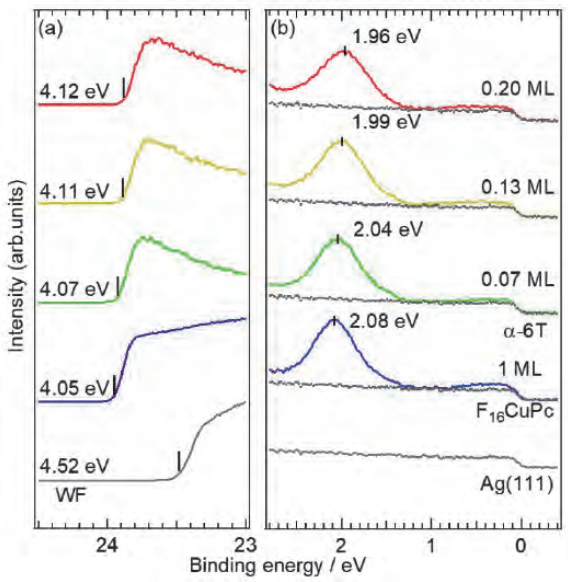

Fig. 1. Evolution of UPS spectra for 6T/F_{16}CuPc interface as a function of 6T coverage.

[1] K. Akaike, A. Onishi, Y. Wakayama and K. Kanai, J. Phys. Chem. C, in press.

[2] J.P. Yang, F. Bussolotti, S. Kera and N. Ueno, J. Phys. D: Appl. Phys. **50** (2017) 423002.

BL3U

Cobalt Oxide Catalyst in Carbonate Aqueous Solution Studied by Operando C K-edge XAFS Measurement

K. Yamada[1], T. Hiue[2], M. Nagasaka[3], H. Yuzawa[3], H. Kondoh[2], Y. Sakata[1] and M. Yoshida[1,4]

[1]*Faculty of Engineering, Yamaguchi University, Ube 755-8611, Japan*
[2]*Graduate School of Science and Technology, Keio University, Yokohama 223-8522, Japan*
[3]*Institute for Molecular Science, Okazaki 444-8585, Japan*
[4]*Blue energy center for SGE technology (BEST), Yamaguchi University, Ube 755-8611, Japan*

In these days, the system to produce hydrogen by water electrolysis utilizing renewable energy such as solar, wind, and salinity concentration gains significant attention due to increasing global awareness of environmental issues. However, the efficiency of water electrolysis is not enough for commercial use, because of the high overvoltage on the oxygen evolution electrocatalyst. In this situation, Takanabe and co-workers reported that cobalt oxide catalyst electrodeposited in carbonate aqueous solution (Co-C_i) could function as the efficient oxygen evolution reaction (OER) catalyst in 2014 [1]. On the other hand, our group find out the function of similar OER catalysts by operando observation using X-ray absorption fine structure (XAFS) technique [2]. Herein, we examined the operando XAFS measurements for Co-C_i catalysts to reveal the function of carbonate species in the Co-C_i.

A Teflon electrochemical cell was equipped with a Pt counter electrode and an Ag/AgCl reference electrode for all electrochemical experiments. The Co-C_i thin films were electrodeposited on Au thin film in potassium carbonate aqueous solution (K-C_i) containing $Co(NO_3)_2$ at 1.7 V vs. RHE. The operando C K-edge XAFS spectra for Co-C_i were taken under electrochemical control with transmission mode at BL3U in the UVSOR Synchrotron, according to the previous works [3].

First, we measured C K-edge XAFS for saturated K_2CO_3 aqueous solution as reference sample (Fig. 1), in order to find out the absorption peak of carbonate species. The absorption peak was estimated around 290.3 eV, corresponding with a previous research about carbonate material [4].

Next, we measured operando C K-edge XAFS spectrum for Co-C_i electrocatalyst. An absorption peak assigned to carbonate adsorbed on the Co-C_i catalyst was observed around 290.4 eV. Moreover, when the electrode potential was changed from 0.5 V to 1.0 V, a new peak was observed around 290.6 eV. In our previous work about operando O K-edge XAFS spectra, we revealed that the CoO_2 structure was generated by the oxidation of CoOOH at higher electrode potential. Therefore, we think the new peak in the C K-edge XAFS is assigned to the carbonate species adsorbed on the CoO_2 structure and functions as the active site for OER process.

In conclusion, we found that the carbonate species were adsorbed on the CoO_2/CoOOH structure in the Co-C_i electrocatalyst by operando C K-edge XAFS and the interface of carbonate/CoO_2 was likely to work as efficient OER site.

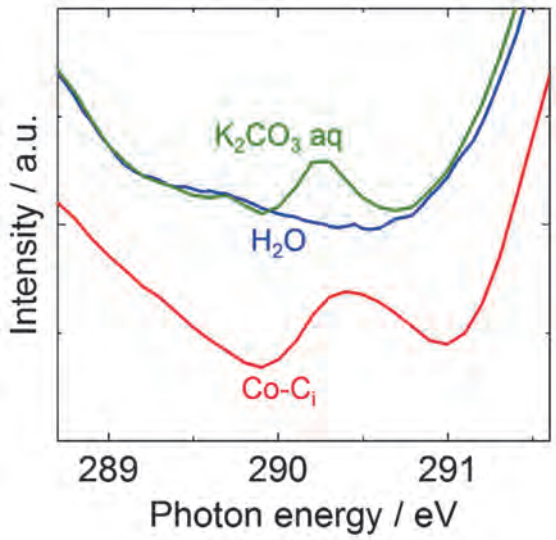

Fig. 1. Operando C K-edge XAFS spectra for the saturated K_2CO_3 aqueous solution (green line) and Co-C_i at 1.7 V vs. RHE (red line).

[1] K. Takanabe *et al.*, Adv. Energy Mater. (2014) 1400252.
[2] M. Yoshida *et al.*, J. Phys. Chem. C **121** (2017) 255.
[3] (a) M. Nagasaka *et al.*, J. Phys. Chem. C **117** (2013) 16343.
(b) M. Yoshida *et al.*, J. Phys. Chem. C **119** (2015) 19279.
[4] Chris Jacobsen *et al.*, J. Synchrotron Rad. **17** (2010) 676.

BL3B

Evaluation of Optical Basic Properties of Ultra-Violet Emitting Zinc Aluminate Phosphor

H. Kominami[1], M. Ohkawa[1], Y. Kato[1], M. Arimura[1], K. Imagawa[1], K. Warita[2], S. Takahashi[2], K. Higashi[2] and S. Nishibori[2]

[1]*Graduate School of Integrated Science and Technology, Shizuoka University, Hamamatsu, 432-8651 Japan*

[2]*Faculty of Engineering, Shizuoka University, Hamamatsu, 432-8651 Japan*

The UV light is used for various applications depending on the wavelength as well as the sterilization described above. The lights of 200-280 nm (UV-C) region as for the sterilization, 280-320 nm (UV-B) region as the treatment of the skin disease, 320-400 nm (UV-A) region as application of purification of water and air, and photocatalysts. Recently, from the viewpoint of consideration to the environment, the mercury free UV emission devices have been demanded for the application of catalyst and medical situations. In our previous work, it was clarified that $ZnAl_2O_4$ phosphor was suitable for the UV field emission lamp because of its stability and luminescent property. It shows strong UV emission peaked around 250 nm which suitable for sterilization.

We are exploring the physical properties of $ZnAl_2O_4$, because the optical properties of $ZnAl_2O_4$ have not been cleared. We tried the evaluation of $ZnAl_2O_4$ using the powder phosphor. However, it is difficult to evaluate because of the influence of surface scattering, such as the absorption coefficient and refractive index reflectance. Therefore, we thought that the thin film analysis was suitable for correct measurements of the fundamental properties. In previous work, $ZnAl_2O_4$ thin film prepared by thermal diffusion process using ZnO film on sapphire substrate. However, the optical measurement was difficult, because the composition of the film and each interface was not uniform.

In this study, to avoid the inarticulate interface of each layer, the multilayer film containing constituent elements was formed by sputtering on sapphire substrate, and tried to prepare the $ZnAl_2O_4$ thin film by thermal diffusion.

In this experiment, we used an RF magnetron sputtering system. Fig.1 shows the experimental procedure of the $ZnAl_2O_4$ film formation. ZnO layer was deposited on a, c, and m-plane sapphire substrates at room temperature. Next, α-Al_2O_3 thin layer was covered with ZnO to avoid re-evaporation by thermal diffusion process because of high evaporation pressure of Zn. All ZnO layer was sandwiched by α-Al_2O_3 layers. The films were annealed at 1000 ºC for several hours in air to enhance thermal diffusion of Zn and Al atoms in the film. The films were evaluated by X-ray diffraction (XRD), scanning electron microscope (SEM), cross-sectional EPMA, and photo- and cathodoluminescence (PL, CL) systems were used.

Figure 1 shows transmittance spectra of $ZnAl_2O_4$ thin film prepared on sapphire substrates annealed at 1000 ºC for 100 hours. The absorption edge of $ZnAl_2O_4$ on a-substrate was sifted to shorter wavelength. For comparison, Fig. 2 shows transmittance spectra of substrates. The change of absorption edge indicates that $ZnAl_2O_4$ film on a-plane substrate was formed Al-rich $ZnAl_2O_4$ spinel structure. From the figure, the interference fringes were also obtained. Now we try to calculate the refractive index from the spectra. We are expecting that the optical parameters of $ZnAl_2O_4$ are obtain from the UVSOR measurement.

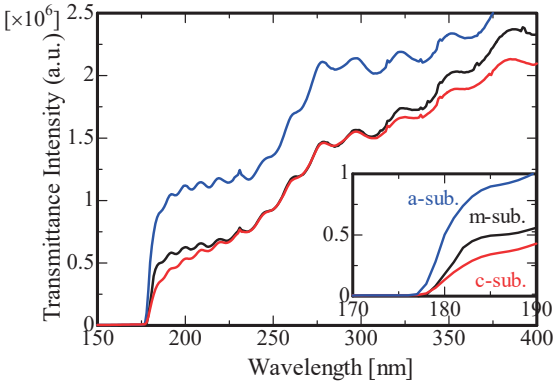

Fig. 1. Transmittance spectra of $ZnAl_2O_4$ thin film prepared on several -plane sapphire substrates annealed at 1000 ºC for 100 hours.

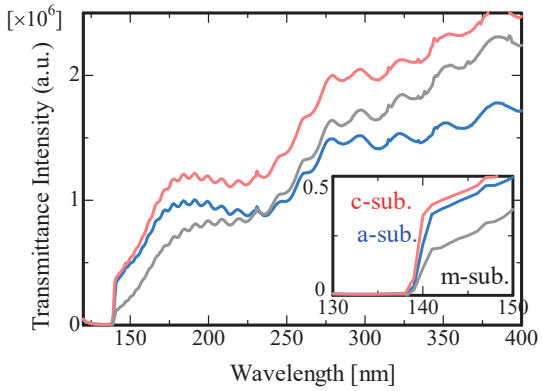

Fig. 2. Transmittance spectra of sapphire substrate.

BL4B, BL5B

Observation of Photoinduced Phenomenon in Amorphous Chalcogenide Thin Films by Ultraviolet Synchrotron Orbital Radiation

K. Hayashi

Department of Electrical, Electronic and Computer Engineering, Gifu University, Gifu 501-1193, Japan

It is well known that amorphous semiconductor materials are very sensitive to the light and show a variety of photoinduced phenomena [1-3]. Therefore, amorphous semiconductor are very expected as materials for optoelectronic devices, such as solar cells, thin film transistors, light sensors, and optical memory devices etc. These applications require an understanding of the physical properties of amorphous materials. In our recent study, we observed interesting photoinduced change in the photoconductivity of amorphous chalcogenide films by the irradiation of the visible light with the energy corresponding to the optical bandgap. To obtain a wide knowledge of the photoinduced phenomena, we are trying to investigate photoinduced effects in the vacuum ultraviolet region by the transmission spectra. In the previous report, we have reported the transmission spectrum of amorphous arsenic selenium thin film measured at beamline BL5B [4, 5]. The inner core level absorption of this material is observed in the wavelength region between 16nm and 30nm. Amorphous thin films for transmission spectrum measurement can be easily prepared by conventional evaporation technique. The aluminum thin film used as a filter for removing higher order light from the monochromator in this wavelength region was used as a substrate for transmission spectrum measurement. However, beamline BL5B does not have very good wavelength accuracy and spectral resolution. Beamline BL4B has better wavelength accuracy and spectral resolution than BL5B, but it is not suitable for measurement in the lower energy region. In this report, we try to measure the transmission spectra of other materials that have absorption levels in the higher energy region and compare the results of BL4B and BL5B.

The metal thin films were prepared onto Corning 7059 glass plates with a pinhole of the diameter of 2.0mm. The transmission spectrum was measured through this pinhole. The metal thin film was used as a filter to eliminate the higher order light from the monochromator in the VUV region and also as a substrate of amorphous film. A gold thin film was used in the wavelength region between 5nm and 12nm, and an aluminum thin film was used in the wavelength region between 16nm and 36nm. A silicon photodiode was used as a detector in the wavelength region. The measurement of the transmission spectra in the VUV region was performed at room temperature at BL4B and BL5B of the UVSOR facility of the Institute for Molecular Science.

Figure 1 shows the transmitted light intensity of metal thin films (Au and Al) measured at BL4B and BL5B by a silicon photodiode. As can be seen in the figure, the transmitted light intensity in the high energy region at BL4B is stronger than at BL5B, which is advantageous for the measurement of the transmission spectrum. In fact, the transmission spectra of amorphous films prepared on gold thin film substrates were able to be measured with higher resolution when measured with BL4B than with BL5B. On the other hand, the transmitted light intensity of the aluminum thin film in the low energy region near 30nm was not much different between the two beamlines. In the measurement of the transmission spectrum in the low energy region, the SN was lower in BL4B than in BL5B.

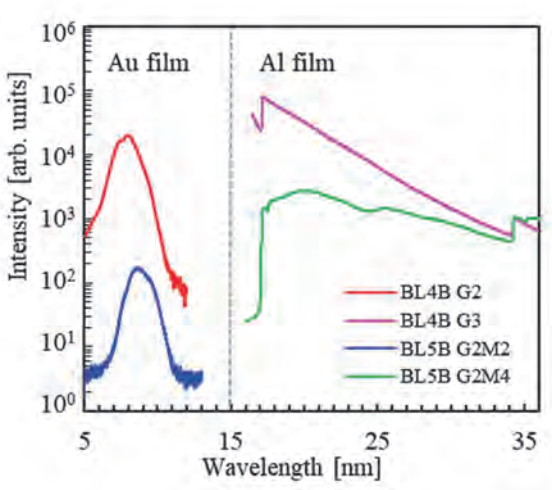

Fig. 1. Transmitted light intensity of thin metal films (Au and Al) measured at BL4B and BL5B by a silicon photodiode.

[1] K. Tanaka, Rev. Solid State Sci. **4** (1990) 641.
[2] K. Shimakawa, A. Kolobov and S. R. Elliott, Adv. Phys. **44** (1995) 475.
[3] K. Tanaka, Encyclopedia of Nanoscience and Nanotechnology **7** (2004) 629.
[4] K. Hayashi, UVSOR Activity Report 2013 **41** (2014) 140.
[5] K. Hayashi, UVSOR Activity Report 2014 **42** (2015) 134.

BL4B

Electronic and Magnetic Properties of FeNi Alloy Thin Films Grown on a Monatomic Layer Magnetic Nitride

T. Miyamachi[1], K. Kawaguchi[1], T. Hattori[1], T. Koitaya[2,3], T. Yokoyama[2,3] and F. Komori[1]
[1]*Institute for Solid State Physics (ISSP), The University of Tokyo, Kashiwa 277-8581, Japan*
[2]*Department of Materials Molecular Science, Institute for Molecular Science, Okazaki 444-8585, Japan*
[3]*Department of Structural Molecular Science, The Graduate University for Advanced Studies (SOKENDAI), Okazaki 444-8585, Japan*

$L1_0$-ordered alloy thin films fabricated by the alternating deposition of magnetic or noble elements attract great attention for their strong uniaxial magnetic anisotropy. Especially, $L1_0$-ordered FeNi alloy thin films, composed of cheap and abundant materials, raise the hope for rare-earth free permanent magnets compatible with NdFeB-based rare earth magnets. Previous studies revealed the close relationship between the strength of the uniaxial magnetic anisotropy and structural ordering. However, the order parameter *S* reported so far still remains low (up to ~ 40 %) for $L1_0$-ordered FeNi alloy thin films and the magnetic easy axis is still along in-plane direction. The low *S* values could be caused by the atomic-scale disorder at the Fe/Ni interface during the fabrication processes, but the lack of the appropriate experimental method with high spatial resolution hampered the intrinsic improvement of structural and resulting electronic and magnetic properties of FeNi alloy thin films.

Toward realizing high quality FeNi alloy thin films, we here focus on the fabrication method utilizing nitrogen surfactant effects in a monatomic layer magnetic nitride. In this method, high lateral lattice stability, which is characteristic of a monatomic layer magnetic nitride [1, 2], and surfactant nitrogen during the deposition of Fe and Ni layers can effectively suppress the interdiffusion at the Fe/Ni interface, leading to atomically flat and homogeneous surface and interface of FeNi alloy thin films.

In this work, we investigate structural, electronic and magnetic properties of 1 monolayer (ML) Fe on a monatomic layer nickel nitride (Ni_2N) grown on Cu(001), the initial stage for the fabrication of FeNi alloy thin films by means of nitrogen surfactant effects, using scanning tunneling microscopy (STM) combined with x-ray absorption spectroscopy/x-ray magnetic circular dichroism (XAS/XMCD). This complementary experimental approach allows to link macroscopic observations of element specific and quantitative electronic and magnetic properties by XAS/XMCD with microscopic origins of the Fe/Ni interface characteristics revealed by STM [3].

The growth of the Ni_2N on Cu(001) was checked by STM before XAS/XMCD measurements. Likewise the fabrication process of a monatomic layer iron nitride (Fe_2N) [1,2], N^+ ions with an energy of 500 eV were firstly bombarded to the Cu(001) substrate and 1 ML Ni was deposited at room temperature. By subsequent annealing at ~ 670 K, well-ordered and flat 1 ML Ni_2N was grown on the surface [4]. 1 ML Fe was thereafter deposited at a low temperature (~ 150 K).

XAS/XMCD measurements were performed at BL4B in UVSOR by total electron yield mode at B = ± 5 T and T = 7.1 K. The XMCD spectra are obtained at the normal (NI: $\theta = 0°$) and the grazing (GI: $\theta = 55°$) geometries by detecting $\mu_+ - \mu_-$, where μ_+ (μ_-) denotes the XAS recorded at Ni and Fe L adsorption edges with the photon helicity parallel (antiparallel) to the sample magnetization. Note that θ is the angle between the sample normal and the incident x-ray.

We find no clear Ni L_3 XMCD signal for bare Ni_2N both in the NI and GI geometries, reflecting its paramagnetic character as previously reported [5]. However, the Ni magnetization is induced by adding 1 ML Fe as a consequence of the formation of Fe_2N/Ni/Cu(001) via nitrogen surfactant effects. The electronic hybridization at the Fe/Ni interface modifies the strong in-plane magnetic anisotropy of Fe_2N [2] toward an out-of-plane direction, but the uniaxial magnetic anisotropy has not yet been achieved.

In future work, combining STM and XAS/XMCD, we will further improve structural ordering of FeNi alloy thin films by annealing and discuss the impacts of surface/interface quality on their electronic and magnetic properties at the atomic scale.

[1] Y. Takahashi *et al*., Phys. Rev. Lett. **116** (2016) 056802.
[2] Y. Takahashi *et al*., Phys. Rev. B **95** (2017) 224417.
[3] S. Nakashima *et al*., Adv. Funct. Mater. **29** (2019) 1804594.
[4] Y. Hashimoto *et al.*, Surf. Sci. **604** (2010) 451.
[5] F. Tanaka *et al.*, J. Appl. Phys. **120** (2016) 083907.

BL4B

Magnetic Coupling at the Interface of Ferromagnetic Iron and Nickel Nitride Monatomic Layers

T. Miyamachi[1], K. Kawaguchi[1], T. Gozlinski[1,2], T. Koitaya[3,4], W. Wulfhekel[2], T. Yokoyama[3,4] and F. Komori[1]

[1]*Institute for Solid State Physics (ISSP), The University of Tokyo, Kashiwa 277-8581, Japan*
[2]*Physikalisches Institut, Karlsruhe Institute of Technology (KIT), Karlsruhe D-76161, Germany*
[3]*Department of Materials Molecular Science, Institute for Molecular Science, Okazaki 444-8585, Japan*
[4]*Department of Structural Molecular Science, The Graduate University for Advanced Studies (SOKENDAI), Okazaki 444-8585, Japan*

$L1_0$-ordered FeNi alloy thin films attract great attention as rare-earth free permanent magnets compatible with NdFeB-based magnets for their expected uniaxial magnetic anisotropy. Previous studies revealed the importance of structural ordering of FeNi alloy thin films on the emergence of the strong uniaxial magnetic anisotropy. However, the order parameter *S* of up to ~ 0.4 reported so far still remains low. The atomic scale disorder could result in the low *S* values, but the details have been overlooked due to the lack of the appropriate experimental method with high spatial resolution. Toward achieving FeNi alloy thin films with high *S* values, we intend to utilize nitrogen surfactant effects in a monatomic layer magnetic nitride, which can effectively suppress the interdiffusion at the Fe/Ni interface and keep atomically flat surface/interface of FeNi alloy thin films.

For this purpose, we have recently performed scanning tunneling microscopy (STM) and x-ray absorption spectroscopy/x-ray magnetic circular dichroism (XAS/XMCD) measurements on a monatomic layer nickel nitride (Ni_2N) on Cu(001) with 1 Fe overlayer, which is the initial stage for the fabrication of FeNi alloy thin films by means of nitrogen surfactant effects. The combined STM and XAS/XMCD study gives the comprehensive information on structural, electronic and magnetic properties of the system both from microscopic and macroscopic points of view. The results demonstrated that nitrogen surfactant effects lead to the formation of a monatomic layer iron nitride (Fe_2N: [1]) on the surface [Ni_2N/Cu(001)→Fe_2N/Ni/Cu(001)], and the strong in-plane magnetic anisotropy of the Fe_2N [2] is partially modified toward the out-of-plane direction. In this work, we further investigate the impacts of annealing on the Fe/Ni interface structures and magnetic properties of the system by STM and XAS/XMCD.

The Ni_2N was grown on Cu(001) by following processes. First, N^+ ions with an energy of 500 eV were bombarded to the Cu(001) substrate and 1 ML Ni was deposited at room temperature. By subsequent annealing at 670 K, well-ordered and flat 1 ML Ni_2N was grown on the surface [3]. The quality of the Ni_2N surface was prechecked by STM and LEED before XAS/XMCD measurements. 1 ML Fe was then deposited on the Ni_2N at 150 K. This "as-deposited sample" was finally annealed up to 420 and 570 K.

XAS/XMCD measurements were performed at BL4B in UVSOR by total electron yield mode at T = 6.1 K and B = 0-5 T. The XMCD spectra are obtained at the normal (NI: $\theta = 0°$) and the grazing (GI: $\theta = 55°$) geometries by detecting $\mu_+ - \mu_-$, where μ_+ (μ_-) denotes the XAS recorded at Ni and Fe L adsorption edges with the photon helicity parallel (antiparallel) to the sample magnetization. Note that θ is the angle between the sample normal and the incident x-ray.

We observed that the XMCD intensity at Fe L_3 edge of the as-deposited sample, Fe_2N/Ni/Cu(001), increases by annealing at 420 K. Furthermore, the magnetization curves of Fe_2N recorded in the NI and GI geometries reveals the enhancement of the magnetic anisotropy. Taking results of atomically resolved STM observations into account, these changes could be attributed to the promotion of the structural ordering at the Fe/Ni interface by annealing at an optimal temperature. In contrast, we found that annealing the as-deposited sample at 570 K degrades magnetic properties of the system. At this annealing temperature, the surface segregation of substrate Cu atoms is activated, locally weakening the magnetic coupling at the Fe/Ni interface.

In the future, we will grow high-quality thicker FeNi alloy thin films by additional alternating Fe and Ni depositions with controlled post-annealing processes, and investigate their structural, electronic and magnetic properties by STM and XAS/XMCD.

[1] Y. Takahashi *et al*., Phys. Rev. Lett. **116** (2016) 056802.
[2] Y. Takahashi *et al*., Phys. Rev. B **95** (2017) 224417.
[3] Y. Hashimoto *et al.*, Surf. Sci. **604** (2010) 451.

BL5U

Valence-Band Electronic Structures of Ultra-Thin Co Layers on Rashba-Splitted Au (111) Surfaces

J. Okabayashi[1,*] K. Tanaka[2] and S. Mitani[3]
[1]*Research Center for Spectrochemistry, The University of Tokyo, Tokyo 113-0033, Japan*
[2]*UVSOR synchrotron Facility, Institute for Molecular Science, Okazaki, 444-8585, Japan*
[3]*National Institute for Materials Science, Tsukuba 305-0047, Japan*

When ferromagnetic transition metals (TMs) are deposited on the Rashba-type spin-orbit coupled surface, novel properties such as perpendicular magnetic anisotropy (PMA) are emerged at the interfaces, which are derived from the symmetry broken spin-orbit effects. The gold Au (111) surfaces have been investigated extensively by means of scanning tunneling microscopy and angle-resolved photoemission spectroscopy (ARPES) because this surface exhibits the large Rashba-type spin-orbit splitting. Large spin-orbit interaction in the heavy element of gold provides the wide varieties for the topological physics and spin-orbit coupled sciences at the surfaces and interfaces. The Rashba splitting of 110 meV in Au (111) surface was reported firstly by LaShell *et al*. [1]. Recently, the interfaces between Au(111) and other heavy elements such as Bi or Ag have been extensively investigated [2, 3]. Here, we focus on the interfaces between ferromagnetic materials and Au(111) interfaces because the thin Fe layers on the heavy elements are expected to exhibit the PMA induced by the Rashba-type spin-orbit interaction.

The spin-orbit coupling between the ferromagnetic 3*d* TMs Fe or Co and 5*d* heavy TM elements of non-ferromagnetic materials such as Pt and Au has been utilized for the PMA through the proximity at the interfaces. It is believed that the future researches concerning not only spins but also orbitals are recognized as the *spin-orbitornics*. Therefore, to clarify the origin of the PMA at these interfaces is a crucial role. The relationship between Au (111) Rashba-type spin-orbit interaction and PMA in 3*d* TMs has not been clarified explicitly. In order to investigate the orbital-resolved states in the Fe films showing the PMA, ARPES at the interfaces becomes powerful techniques through the photon-energy and polarization dependences in each 3*d* orbital. By using ARPES, we aim to understand the orbital-resolved electronic structures at the magnetic interfaces on the Rashba-type Au (111) surface in order to develop the researches of novel PMA using spin-orbit coupled interfaces.

We prepared the clean Au (111) surface for the Co deposition. The commercialized single-crystalline 100-nm-thick Au (111) films on Mica were used. At the beamline BL5U in UVSOR, we repeated the Ar-ion sputtering at 1 kV accelerating voltage and subsequent annealing at 400 °C under the high vacuum conditions. After the sample preparation, the Co layer was deposited at room temperature and then annealed. By *in-situ* transferring the samples into the ARPES chamber, we performed ARPES at 10 K using the photon energies of 60 and 120 eV because of the large cross-section of Au (111) surface states and detections of Co 3*s* and Au 4*f* intensity ratios, respectively.

Figure 1 displays the Co deposition dependence on Au (111). As shown in Fig. 1a, the intensity ratio between Co 3*s* and Au 4*f* peaks systematically changes. The Au (111) surface clearly exhibits the Rashba-type surface states. The Co 3*d* states appear near the Fermi level (E_F) and the surface states disappear. As shown in Fig. 1b, k_x-k_y plots taken by horizontal and vertical polarized beams exhibit asymmetric feature, which can be explained by the Co 3d orbital resolved states through the overlap between Co and Au. Furthermore, we confirmed the PMA at Co/Au interface by x-ray magnetic circular dichroism. Therefore, the interfacial chemical reaction between Co and Au brings the novel properties on the ultrathin Co electronic structures.

We acknowledge Dr. S. Ideta in IMS for technical supports of data analyses. This work was in part supported by KAKENHI Kiban(S) project.

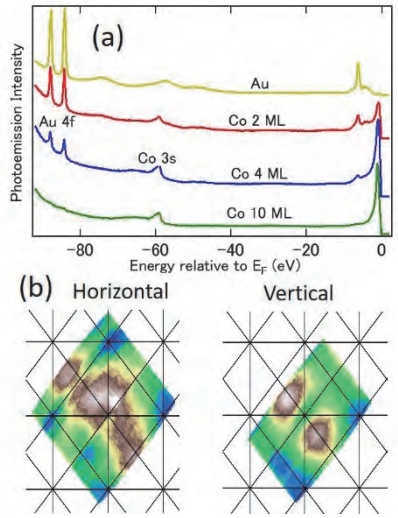

Fig. 1. (a) Photoemission spectra for various Co deposited layers taken at 120 eV. (b) Polarization-dependent k_x-k_y Fermi surface mapping of Co 4 ML taken at 60 eV.

[1] S. LaShell *et al.*, Phys. Rev. Lett. **77** (1996) 3419.
[2] C. Tusche *et al.*, Ultramicroscopy **159** (2015) 620.
[3] B. Yan *et al.*, Nature Commun. **6** (2015) 10167.

*e-mail: jun@chem.s.u-tokyo.ac.jp

BL5U

Effects of P Segregation on the Surface Electronic Structure of $Fe_2P(0001)$

N. Maejima[1,2], Y. Sugizaki[1], Y. Shimato[1], T. Yoshida[1] and K. Edamoto[1,2]
[1]*Department of Chemistry, Rikkyo University, Tokyo 171-8501, Japan*
[2]*Research Center for Smart Molecules, Rikkyo University, Tokyo 171-8501, Japan*

Transition metal phosphides (TMPs) are good candidates for the catalyst in the next generation for hydrodesulfidation. Although Ni_2P shows the highest catalytic activity among TMPs, Fe_2P, which have the same crystal structure as that of Ni_2P, shows the lowest catalytic activity.[1] One of possible origins of the activity difference is the difference in the surface electronic structures of these catalysts. We have reported that surface segregation of P atoms in Ni_2P induces the change of surface electronic structure in the vicinity E_F.[2, 3] On the other hand, P segregation in $Fe_2P(10\text{-}10)$ had little effect on the surface electronic structure around E_F.[4] In this study, we investigated the process of P segregation induced by annealing and its effect on the electronic structure of $Fe_2P(0001)$ using photoelectron spectroscopy (PES) at BL5U, and the results will be compared with those of Ni_2P.

Figure 1 shows the peak intensity ratio of P_{LMM} to Fe_{MVV} obtained by Auger electron spectroscopy (AES) in various conditions of annealing temperature. The ratio decreased by annealing at temperatures lower than 400 °C and increased with annealing at higher than 400 °C. It indicates that the surface segregation induced by the annealing at higher than 400 °C. The P segregation process was studied in detail by P *2p* PES. Figure 2 show the results of the fitting of the P *2p* spectrum of $Fe_2P(0001)$ clean surface. The spectrum can be fit with seven P components. The inspection of annealing temperature dependence of each peak shows that a,b,d,f and g components are increased in intensity by annealing at higher than 350 °C, while those of c and e components are decreased by annealing at higher than 350 °C. PES and AES results indicate that segregation and desorption of P atoms compete at 350 °C and segregation exclusively proceeds at higher than 400 °C. Finally, we studied the change of surface electronic structure by the heating treatment. Figure 3 shows the valence band spectra of $Fe_2P(0001)$ annealed at various temperatures at 300 – 700 °C. All spectra are normalized by the peak top intensity at 0.2 eV. Although the spectral line shape in the range of 1 - 4 eV is changed by annealing, the peak in the vicinity of the E_F did not show any shifts. These results indicate that segregated P atoms have little effect on the surface electronic structure around E_F of $Fe_2P(0001)$. Although the Ni 3d states are stabilized through the segregating P atoms for the Ni_2P, the Fe 3d states are not changed by P segregation for Fe_2P, which would be one of the possible origins of the stark contrast in the catalytic activities of these materials.

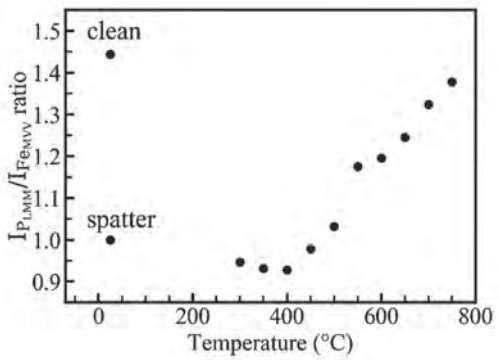

Fig. 1. The results of Auger electron intensity ratio at each annealing temperature.

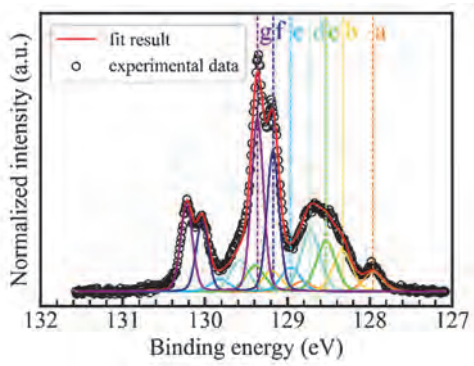

Fig. 2. Fitting result of P *2p* spectra obtained from clean surface of $Fe_2P(0001)$.

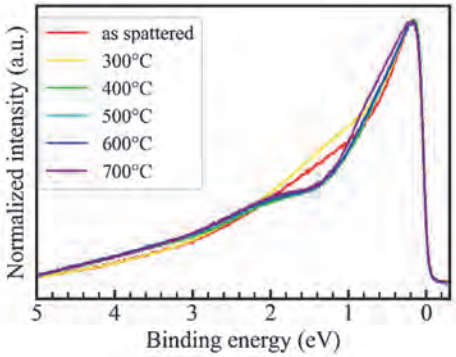

Fig. 3. The change of valence band spectrum obtained from the sample annealed at each temperature.

[1] S. T. Oyama *et al*., Catal Today **143** (2009) 94.
[2] K. Edamoto *et al*., Appl. Surf. Sci. **269** (2013) 7.
[3] S. Ishida *et al*., e-J. Surf. Sci. Nanotech. **13** (2015) 93.
[4] Y. Sugizaki *et al*., Jpn. J. Appl. Phys. **57** (2018) 115701.

BL5U

Measuring the Berry Curvature of Dresselhaus Semiconductor by Circular Dichroism ARPES

S. Cho[1], D. Oh[2,3], K. Tanaka[4], S. R. Park[5] and C. Kim[2,3]

[1]*Institute of Physics and Applied Physics, Yonsei University, Seoul 03722, Korea*
[2]*Center for Correlated Electron Systems, Institute for Basic Science (IBS), Seoul 08826, Republic of Korea*
[3]*Department of Physics and Astronomy, Seoul National University (SNU), Seoul 08826, Republic of Korea*
[4]*UVSOR Synchrotron Facility, Institute for Molecular Science, Okazaki 444-8585, Japan*
[5]*Department of physics, Incheon National University, Incheon 406-772, Korea*

Recently, Datta and Das [1] proposed that spin-field-effect transistor (spin-FET) can be shown by in light of controllability of spin precession motion of electrons of zinc blende semiconductors (ZBS) [2, 3, 4]. The ZBS have unique features; broken inversion symmetry and strong spin orbit coupling (SOC). The features lead to an effective momentum dependent magnetic field which lifts the spin degeneracy of the electrons in the materials. The helical spin structure can be described successfully by Rashba and Dresselhaus model at a constant energy contour of the valence band [5]. The unique spin structure lead to the noble spin transport, spin Hall effect, and this was shown by Kerr rotation measurement in GaAs with zinc blende structure enerally imply that there is a transvers velocity which proportional to the Berry curvature [6, 7]. Understanding the Berry curvature of the ZBS is considered important to develop the spin-FET.

In this study, we try to inverstigate the Berry curvature of HH and LH band of ZBS. We note that the semiconductor with zinc blende structure generally have the three hole bands which consist of 2-fold degenerate (j = 1/2) and 4-fold degenerate (j = 3/2) state, resulting from the SOC and a negligible crystal field. The j = 3/2 state split into heavy- ($m_J = \pm 3/2$) (HH) and light hole ($m_J = \pm 1/2$) (LH) bands near the Fermi level. The j = 1/2 state, called split-off band, is located at a higher binding energy about the energy splitting (Δ) than j = 3/2 state. This splitting Δ is determined by the magenitude of the spin-orbit interaction. Since the HH and LH state have different value of m_J, it is expected that the Berry curvature have different behavior [8].

To show the Berry curvature of Bloch state in the ZBS, we note a recent proposal, based on the study on the relation bewteen Berry curvature and circular dichroism (CD)-ARPES, that the CD-signal is approximatly proportional to the Berry curvature in 2H-WSe_2 [9]. It implied that CD-ARPES can show the Berry curvature of Bloch state in momentum space. From the previous study, it is expected that the diffetent behavior of the Berry curvature between HH and LH state can be shown by CD-ARPES measurement.

Figures 1(a) and (b) show the ARPES intensity map of InSb at a binding energy 0.6 eV obtained from righ-(RCP) and left (LCP) circularly polarized light. Then, we can have CD-signal, as shown in Fig. 1(c), from the difference between the intensity map taken from RCP and LCP light. In our result as depicted in Fig. 1(c), outer (inner) band indicate the CD-intensity map of HH (LH) band. But, they seem to illustrate a similar CD-pattern. We think that our CD-intensity map refleced the final state effect because CD-ARPES data of HH and LH band were taken with 2nd Brillouin zone (BZ). In that experiments, since the ARPES intensities with RCP and LCP light in first BZ were too low, we chose the 2nd BZ.

[1] S. Datta *et al.,* Appl. Phys. Lett. **56** (1990) 665
[2] Y. A. Bychkov *et al.,* JETP Lett. **39** (1984) 78.
[3] J. Schliemann *et al.,* Phys. Rev. Lett. **90** (2003) 146801.
[4]X. Cartoixà *et al.,* Appl. Phys. Lett. **83** (2003) 1462.
[5] G. Dresselhaus, Phys. Rev. **100** (1955) 2.
[6] S. Murakami *et al.*, Science **301** (2003) 1348.
[7] Y. K. Kato *et al*., Science **306** (2004) 1910.
[8] M.-C. Chang and Q. Niu, J. Phys.: Condens. Matter **20** (2008) 193202.
[9] S. Cho *et al.*, PRL **121** (2018) 186401.

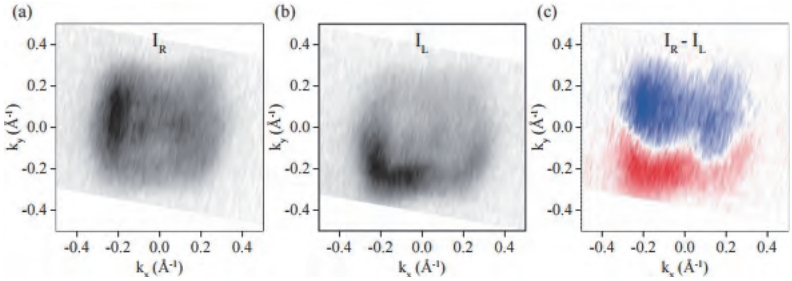

Fig. 1. ARPES intensity map of InSb at a binding energy 0.6 eV taken with (a) right and (b) left circularly polarized 70 eV light. (c) Circular dichroism (CD) intensity obtained from the difference between (a) and (b).

BL6U

Arpes Study of $(Bi_xSb_{1-x})_2Se_3$ Topological Insulators

L. Yashina[1] and F. Matsui[2]

[1]*Chemistry Department, Moscow State University, Moscow 119991, Russian Federation*

[2]*UVSOR Synchrotron Facility, Institute for Molecular Science, Okazaki 444-8585, Japan*

Band structure of crystals of a series of solid solutions $(Bi_xSb_{1-x})_2Se_3$ (x=1 - 0.7) between prototypical topological insulator (TI) Bi_2Se_3 [1] and trivial insulator (BI) Sb_2Se_3 was studied by means of ARPES. In the Bi_2Se_3-Sb_2Se_3 system, topological phase transition was predicted theoretically. In this project we have aimed on revealing its relevant aspects: spontaneous destroying or gap formation in Dirac cone and x composition corresponding to topological phase transition. For better surface sensitivity photon energy hv=60 eV was chosen.

Increasing an antimony content leads to Dirac point shifting towards bulk valence band at range x=1-0.8. This trend breaks at $(Bi_{0.7}Sb_{0.3})_2Se_3$ composition (Fig.1a). In case of its electronic structure, Dirac point is located approximately at the same energy that in Bi_2Se_3 (Fig.1a). However, exact energy position of Dirac point in at $(Bi_{0.7}Sb_{0.3})_2Se_3$ is hard to estimate. Bisthmus-like band structure near Dirac point allowed us to suggest, that backscattering channels starts to open near the $(Bi_{0.7}Sb_{0.3})_2Se_3$ composition, but no energy gap in topological surface state was not observed (Fig.1b).

[1] Y. Xia *et al*., Nat. Phys. **5** (2009) 398.

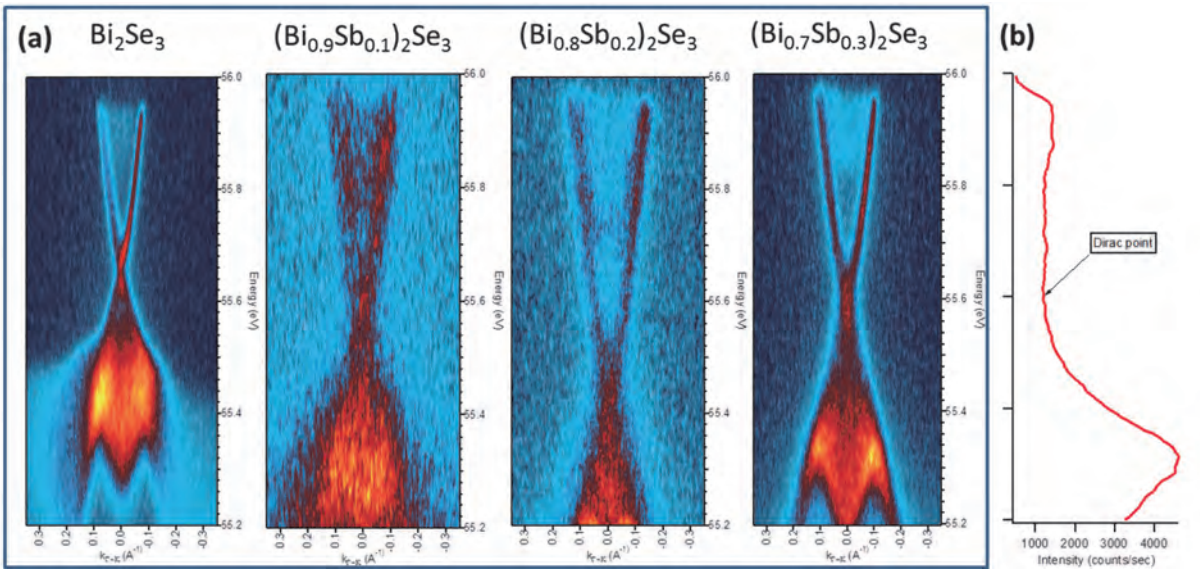

Fig. 1. a) Energy dispersion curves along K-Γ-K direction as a function of crystal composition. b) Constant momentum cross-section at $k_{\Gamma\text{-}K}$=0 for $(Bi_{0.7}Sb_{0.3})_2Se_3$ compound.

BL6U

Reversible and Irreversible Metal-insulator Transition of VO_2

T. Zhai[1], J. Yang[1], F. Matsui[2] and S. Duhm[1]

[1]*Institute of Functional Nano & Soft Materials (FUNSOM), Soochow University, Suzhou 215123, P. R. China*

[2]*UVSOR Synchrotron Facility, Institute for Molecular Science, Okazaki 444-8585, Japan*

Vanadium Dioxide (VO_2) is widely known for its first order metal-insulator transition (MIT) property. The MIT goes along with a structural change from a monoclinic phase to a rutile phase at 340 K, while the conductivity increases 5 orders of magnitude comparing to the insulating phase. Moreover, also oxygen vacancies [1] or soft X-ray irradiation [2] can lead to a metallic state.

Figure 1 shows the electronic structure of insulating and metallic VO_2 based on a previous photoelectron spectroscopy (PES) study [3]. For insulating VO_2 the occupied V 3d derived orbital (termed as $d_{\|}$) is located below the Fermi level, while the other two V 3d orbitals, $d_{\|}^*$ and π^*, are unoccupied and provide a 0.6 eV band gap. In the metallic phase the $d_{\|}$ and π^* orbitals are partially filled. Interestingly, non-stoichiometric $VO_{2-\delta}$ shows a similar behavior. However, the details of the electronic structure are not clarified yet. Especially the unoccupied DOS of $VO_{2-\delta}$ is largely unexplored. Thus, we performed X-ray absorption spectroscopy (XAS), resonant photoemission (RPES) and ultraviolet photoelectron spectroscopy (UPS) experiments at BL6U.

VO_2 thin films were fabricated by pulsed laser deposition (PLD) [1,3] and cleaned by sputtering and annealing cycles in the ultra-high vacuum (UHV) preparation chamber of the BL6U endstation. The stoichiometry can be controlled by annealing at 423 K in UHV (base pressure: ~8 x 10^{-10} mbar) or in partial oxygen atmosphere (~9 x 10^{-5} mbar).

The XAS spectra in Fig. 2 show the V L-edge and the O K-edge regions of pristine, stoichiometric VO_2 at room temperature (RT), the sample after an exposure to X-rays of 180 min and a pristine VO_2 sample at 388 K. The peak shift at the V L_3 edge at ~511.6 eV is ascribed to the weight increase of t_{2g} due to the irradiation, which also narrows the band gap; the t_{2g} of O K-edge region from irradiation induced VO_2 exhibits weight loss. In the meantime the energy interval between the t_{2g} and e_g becomes smaller. UPS (not shown) confirms a metallic state of irradiated VO_2. The irradiation induced phase is different to the temperature induced metallic phase. In particular, the main absorption peak at the V L-edge shift does not show an apparent shift. The O K-edge absorption features reveal that there is almost no oxygen loss during the temperature induced reversible MIT.

In conclusion, our preliminary data analysis confirms that X-ray exposure of VO_2 leads to a non-reversible phase transition and to a metallic state at RT. Analyzing the additional XAS data and the RPES and UPS data measured at BL6U, will allow us to understand the mechanism leading to this phase transition. Moreover, our data will also shed light on the electronic structure of VO_2 upon the temperature and the oxygen vacancy induced MIT.

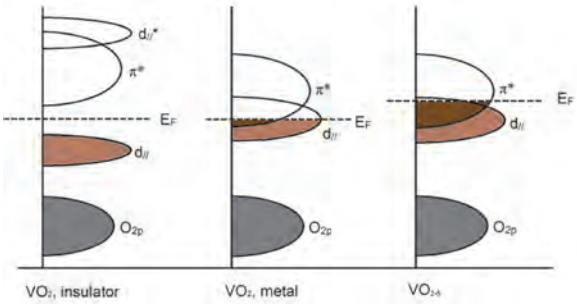

Fig. 1. Electronic structure of stoichiometric VO_2 (insulating and metallic phase) and $VO_{2-\delta}$. In the insulating state a gap opens between the V 3d derived $d_{\|}^*$, π* and $d_{\|}$ orbitals. Taken from Ref. [3].

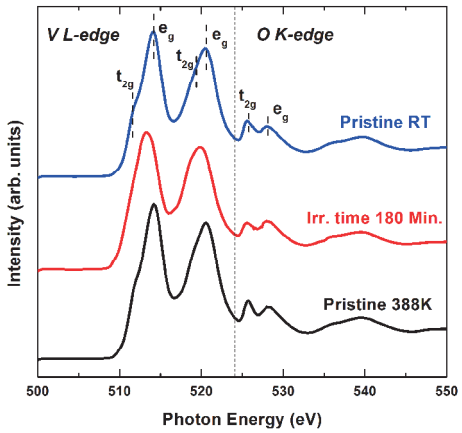

Fig. 2. XAS spectra for pristine VO_2 at RT, the same sample after 180 minutes of X-ray exposure and pristine VO_2 at 388 K. In all cases, the V L-edge region and the O K-edge region are shown. The peaks are labeled according to Ref. [4].

[1] R.-B. Wang, T. Katase, K.-K. Fu, T.-S. Zhai, J.-C. Yang, Q.-K. Wang, H. Ohta, N. Koch and S. Duhm, Adv. Mater. Interfaces **5** (2018) 1801033.

[2] V. R. Singh, V. Jovic, I. Valmianski, J. G. Ramirez, B. Lamoureux, I. K. Schuller and K. E. Smith, Appl. Phys. Lett. **111** (2017) 241605.

[3] K.-K. Fu, R.-B. Wang, T. Katase, H. Ohta, N. Koch and S. Duhm, ACS Appl. Mater. Interfaces **10** (2018) 10552.

[4] R. Zimmermann, R. Claessen, F. Reinert, P. Steiner and S. Hüfner, J. Phys.: Condens. Matter **10** (1998) 5697.

.

BL6U

Resonant Photoemission Spectroscopy of Aligned Graphene Nanoribbons

D. Usachov[1], B. Senkovskiy[2] and F. Matsui [3]

[1]*Saint Petersburg State University, 7/9 Universitetskaya Nab., St. Petersburg 199034, Russia*
[2]*II. Physikalisches Institut, Universität zu Köln, Zülpicher Strasse 77, 50937 Köln, Germany*
[3]*UVSOR Synchrotron Facility, Institute for Molecular Science, Okazaki 444-8585, Japan*

Absence of a band gap in graphene prevents its wide use in electronic devices. This problem can be overcome by reducing dimensionality from 2D to 1D. Due to quantum confinement graphene nanoribbons (GNRs) have a notable band gap and a tunable electronic structure, and therefore they are a promising material for optoelectronic applications. Furthermore, thanks to the bottom-up nanofabrication technique it is possible to synthesize atomically precise GNRs with defined electronic properties. GNRs also represent significant fundamental interest because of being an intermediate system between a 2D crystal and molecules. Their valence band is formed by a set of subbands possessing dispersion along the ribbon axis, while in perpendicular direction the wave function is trapped in a narrow quantum well [1]. Bottom-up synthesis allows atomically precise fabrication of GNRs of fixed width. The present work is devoted to resonant photoemission study of 7-atom-wide armchair-edge GNRs (7-AGNRs) aligned on a stepped Au(788) surface.

The C K-edge NEXAFS spectrum of 7-AGNR contains fine features, which can be associated with different unoccupied subbands [2]. Therefore, it was expected that photoemission from different subbands could be selectively enhanced by tuning the photon energy near the absorption resonance.

Figure 1 shows preliminary results of our study. The upper row corresponds to such tilting angle of sample, at which the topmost valence subband (indicated by the arrow) has maximal intensity. At the photon energy of 284.6 eV, which is just below the absorption edge, this subband is not visible because of low photoemission cross section. When the photon energy is increased to 285 eV the subband is resonantly enhanced (shown with white arrow). However, already at 285.8 eV it disappears.

The second row corresponds to the second subband. We have found that its behavior is different from the first one. While it is resonantly enhanced at 285 eV, it does not disappear at 285.8 eV. For the third subband (shown in the third row) the resonance seems to be shifted to higher photon energies. This is a clear indication that different valence subbands are selectively excited with photons of different energy at the C absorption K-edge. Further theoretical calculations will be performed to understand this effect in more detail.

Another result of our study was the discovery of the fact that 7-AGNRs undergo radiation damage when the photon energy is set to the C K-edges absorption resonance. The valence bands rapidly vanish under the photon beam. We suppose that photoexcited nanoribbons undergo dehydrogenation and become chemically active due to formation of carbon dangling bonds. Such active edge carbon atoms may react with adsorbates. This opens a possibility for chemical functionalization of GNRs by means of photostimulated reactions. This possibility will be explored in more detail in the future experiments.

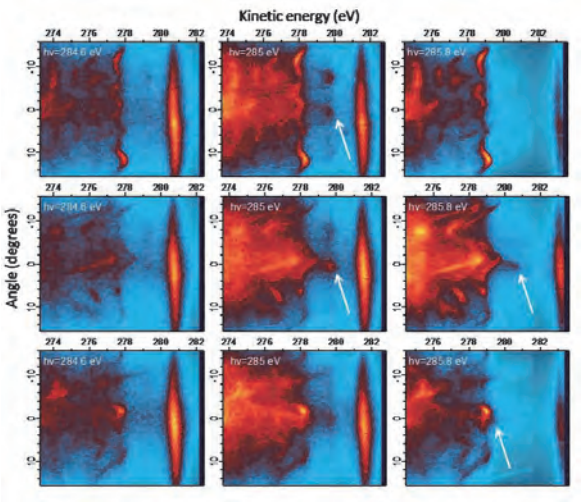

Fig. 1. Resonance photoemission of 7-AGNR at the carbon K-edge. Different rows correspond to different sample orientations at which different subbands exhibit the highest intensity.

[1] B. V. Senkovskiy *et al.,* 2D Mater. **5** (2018) 035007.
[2] B. V. Senkovskiy *et al.,* ACS Nano **12** (2018) 7571.

BL6U

Photoemission Tomography of Organic Monolayer: Substrate-assisted Intermolecular Dispersion of PTCDA on Cu(100)

A. Haags[1,2], M. Meissner[3], X. Yang[1,2], F. Matsui[3], S. Soubatch[1,2], F. S. Tautz[1,2] and S. Kera[3]
[1]*Peter Grünberg Institut (PGI-3), Forschungszentrum Jülich, 52425 Jülich, Germany*
[2]*Jülich Aachen Research Alliance, Fundamentals of Future Information Technology, 52425 Jülich, Germany*
[3]*UVSOR Synchrotron Facility, Institute for Molecular Science, Okazaki 444-8585, Japan*

The transport properties of electronic materials are crucial for device performances. This is particularly important for organic-based electronics [1, 2], because charge mobility in molecular films is usually restricted due to a hopping transport, while exclusively band-like transport along the π stacking direction is expected in well-structured films. However, recently several reports have been published about intermolecular band dispersion of occupied states in the organic monolayers on metal in the lateral direction. Since there is no significant overlap of π states, the rise of dispersion in these cases has been attributed to molecule-substrate hybridization. An example is the strong intermolecular dispersion of the former lowest unoccupied molecular orbital (f-LUMO) of perylene-tetracarboxylic dianhydride (PTCDA) on Cu(100) [3]. Upon PTCDA adsorption on Cu(100), its LUMO becomes occupied due to the charge transfer from copper and forms a dispersive band whose momentum-space (*k*-space) pattern clearly reflects the symmetry of the PTCDA/Cu(100) interface [3].

An intriguing aspect in this context is the *k*-space character of the hybridized molecular electronic states. Recently it has been shown by means of photoemission tomography that the *k*-space patterns of particular molecular states usually retain their shapes despite hybridization and charge transfer [4]. Only in case of the dispersive mixed state, the modified symmetry of wave-functions becomes apparent in the *k*-space patterns as an additional fine-structure [3, 5]. So far it remains unclear, why the symmetry of the hybridized molecular states changes in some cases and remains intact in others. To shed light on this issue, a combined experimental and theoretical approach is required. The experimental setups used so far for photoemission tomography, such as *k*-space imaging photoemission microscopes and a toroidal electron spectrometer, suffer from poor energy and *k*-space resolution, which is particularly needed for a characterization of dispersive bands. On the other hand, the analytical tools providing state-of-the-art resolution, for example hemispherical analyzers, do not have the *k*-space imaging option.

To address this issue, we initiated a series of experiments using the two-dimensional (2D) angle-resolved photoemission end-station based on an MBS A-1 hemispherical electron analyzer with modified lens system at the BL6U beamline of UVSOR. The 2D *k*-space resolution in this case is achieved by a mechanical deflection of the lens system perpendicular to the entrance slit of the analyzer. Correspondingly, the photoemission distribution is recorded as a set of energy distribution maps depending on the deflection angle resulting in a three-dimensional dataset I(E_{kin}, φ, θ).

To demonstrate the capability of the setup for photoemission tomography applications, we grew a commensurate monolayer of PTCDA on Cu(100) and carried out angle-resolved photoemission spectroscopy at room and low temperature. To visualize the experimental results, we developed a python-based software. The 2D angle-space resolved photoemission patterns measured at the binding energy corresponding to the f-LUMO, clearly resemble the contrast of the major LUMO emission lobes as well as substrate-related features - copper *sp*-bands.

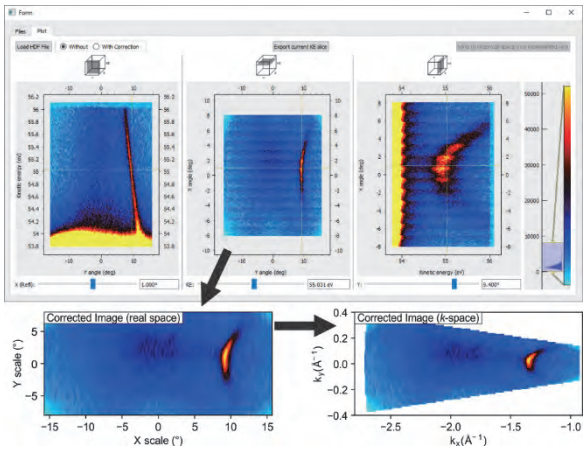

Fig. 1. Screenshot of the python-based software for data evaluation. Top: slicing in different axes of the 3D data cube I(E_{kin}, φ, θ) measured on PTCDA/Cu(100); Bottom Left: corrected I(φ, θ) image for E_{kin} = 55 eV; Bottom Right: corresponding image converted to reciprocal space.

[1] M. Schwarze *et al.*, Nat. Mat. **18** (2019) 242.
[2] N. Ueno and S. Kera, Prog. Surf. Sci. **83** (2008) 490.
[3] D. Lüftner *et al.*, Phys. Rev. B **96** (2017) 125402.
[4] S. Weiss *et al.*, Nat. Commun. **6** (2015) 8287.
[5] T. Ules *et al.*, Phys. Rev. B **90** (2014) 155430.

BL7U

Fabrication of Bi_1Te_1 Ultrathin Films and the Surface Electronic Structure

S. Kusaka[1], K. Yokoyama[1], S. Ideta[2], K. Tanaka[2], S. Ichinokura[1] and T. Hirahara[1]
[1]*Department of Physics, Tokyo Institute of Technology, Tokyo 152-8551, Japan*
[2]*UVSOR Synchrotron Facility, Institute for Molecular Science, Okazaki 444-8585, Japan*

A typical example of a compound composed of Bi and Te is Bi_2Te_3 (Te-Bi-Te-Bi-Te), which is known as a strong topological insulator (TI), but compounds having different composition ratios also exist. One of them, Bi_1Te_1, is a superlattice (Te-Bi-Te-Bi-Te - Bi-Bi-Te-Bi) in which two Bi_2Te_3 quintuple layer (QL) and one bilayer (BL) of Bi stack alternately [1]. There can be three types of terminations for this material, namely 1QL and 2QL Bi_2Te_3 terminations or a BL-Bi termination. It is called a dual TI and has a surface state of a topological crystal insulator (TCI) which is protected by the mirror symmetry of a crystal and a surface state of a weak topological insulator protected by time reversal symmetry. They are located at different surface orientations. Thus it has been predicted that Bi_1Te_1 can realize novel exotic properties by breaking individual symmetries protecting different topologies by applying a magnetic field or a lattice distortion and inducing a gap in the respective surface Dirac cone [2].

In the previous study, Bi_1Te_1 was prepared by depositing Bi and Te at a ratio of 1:1 with molecular beam epitaxy (MBE), and its electronic structure was reported [2]. However, the surface termination seemed to be mixed between 1QL and 2QL Bi_2Te_3. Therefore, for a better understanding of Bi_1Te_1, establishment of a stable sample preparation method with a well-defined surface termination is required. Therefore in the present study, we tried to fabricate a Bi_1Te_1 thin film with controlled termination by a different method. Namely, first we fabricated Bi_2Te_3(111) films by depositing Bi and Te at a ratio of 1:5 with MBE (Fig. 1 (a)) and then annealed it to get rid of Te layers. The samples thus prepared showed three different band dispersions as shown in Fig. 1 (b-d) before breaking. We found through comparison with *ab initio* calculations for Bi_1Te_1 with different surface terminations that (b) showed similarities with the 2QL-Bi_2Te_3 terminated Bi_1Te_1, whereas (d) was similar to the 1QL-Bi_2Te_3 terminated Bi_1Te_1, although there was no quantitative match [2]. (c) was identified as an intermediate state of (a) and (b). Furthermore, we also observed a Dirac point in the direction perpendicular to Γ-M at a wavenumber not equal to zero (Γ point). This was also seen in the theoretical calculation and thus this (111) surface was identified as the surface possessing the TCI Dirac cone.

We are now trying to investigate the real atomic structure of this system with low-energy electron diffraction (LEED) as well as cross sectional transmission emission microscopy (X-TEM). There is a possibility that they are not actually Bi_1Te_1, but rather more complex structures composed of BL-Bi and Bi_2Te_3, such as Bi_4Te_5, Bi_6Te_7, Bi_4Te_3, Bi_2Te, Bi_7Te_3 [3]. In any case, the combination of ARPES, ab initio calculations, and structure analysis should be very useful in studying the topological properties of Bi-Te compounds.

[1] T. Hirahara *et al.,* Phys. Rev. Lett. **107** (2011) 166801.
[2] M. Eschbach *et al.,* Nat. Comm. **8** (2017) 14976.
[3] O. Concepcion *et al.,* Inorg. Chem. **57** (2018) 10090.

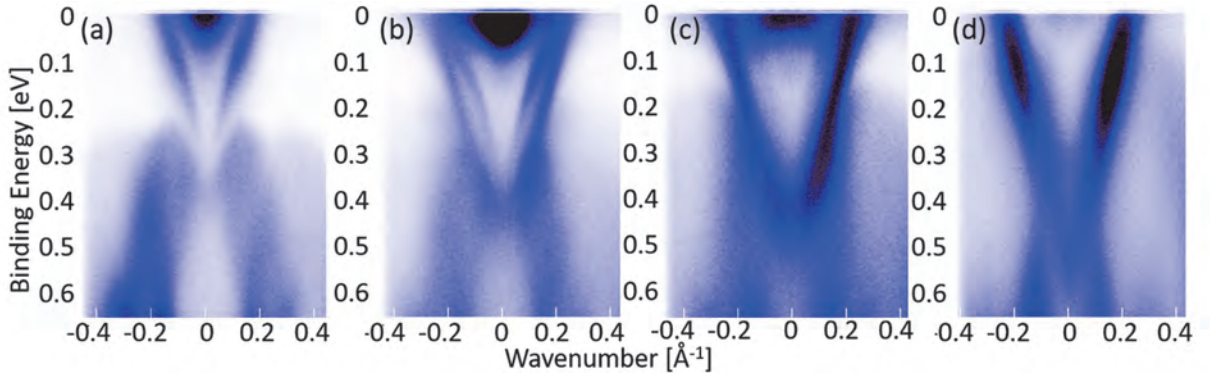

Fig. 1. Band dispersion of Bi_2Te_3 (a) and that obtained by annealing it (b-d), which is likely Bi_1Te_1 with different surface terminations. The measurements were performed along the Γ-M direction.

BL7U

Photoelectron Angular Distribution of Pentacene/Graphite Interface Investigated by Low-energy Angle-resolved Photoelectron Spectroscopy

T. Yamaguchi[1,2], M. Meissner[2], S. Ideta[1,3], K. Tanaka[1,3] and S. Kera[1,2,3]

[1]*School of Physical Sciences, The Graduate University for Advanced Studies (SOKENDAI), Okazaki 444-8585, Japan*
[2]*Department of Photo-Molecular Science, Institute for Molecular Science, Okazaki 444-8585, Japan*
[3]*UVSOR Synchrotron Facility, Institute for Molecular Science, Okazaki 444-8585, Japan*

Ultraviolet photoelectron spectroscopy (UPS) is a very useful technique for studying the electronic structure of surfaces and interfaces. However, the origin of UPS features obtained by low-energy photon excitation is not well established theoretically and experimentally because of the complicated photoemission process. Tanaka et al. demonstrated resonance excitation between initial states and final states which causes unexpected scattering due to the relatively long lifetime of low-energy electrons potentially trapping them in intermediate states at the interface [1]. A similar behavior was found for organic monolayers on graphite, giving rise to inelastic energy-loss features [2-4]. In addition, the lifetime of photogenerated holes may also lead to interesting phenomena. Franck-Condon anomalies, where the vibronic progression does not follow that of the gaseous phase and shows a strong angular anisotropy, and photoemission matrix anomalies, where high intensity appears at the surface normal, were observed for monolayers of flat-lying organic molecules on graphite [2-4]. Moreover, anomalous bands have been reported, caused by conduction bands in the secondary electron emission (SEE) background [5]. Therefore, despite the weak interaction of physisorbed molecules with the substrate, the corresponding wavefunctions may connect strongly at the interface; and the combination of these effects could be used to study the impact on the electronic states. In this work, we investigated the photoelectron angular distribution (PAD) of the highest occupied molecular orbital (HOMO) for pentacene (PEN), using low-energy angle-resolved UPS (LE-ARUPS) to clarify those phenomena.

Highly oriented pyrolytic graphite (HOPG) as the substrate was cleaned by annealing at 600 K for 2 h. A PEN film of 4 Å was deposited on HOPG at room temperature in a custom UHV chamber designed for organic layer deposition.

Figure 1(a) shows a LE-ARUPS map taken at $h\nu$ = 7.7 eV and T = 15 K. In the HOMO region (1.6 ~ 2.0 eV) some features stand out: (i) Strong photoemission intensity around the Γ point which is unexpected for p-polarized excitation of weakly bounded, flat-lying, pi-conjugated molecules, (ii) the first vibronic satellite has a higher intensity at Γ than the HOMO (dashed oval in Fig. 1(a)), which deviates from the spectral shape found for higher photon energies such as HeI light, and (iii) a faint background in form of a strongly dispersed dark band and/or bright bands with constant kinetic energy is detected (dashed straight lines). The latter can be seen more clearly when averaging LE-ARUPS maps for different photon energies (here 7.4 ~ 7.8 eV) and normalizing the averaged map by its horizontally and vertically integrated profiles separately (Fig. 1(b)). This way, a constant-kinetic-energy feature becomes more prominent while molecular occupied states move in energy and "scan" the unoccupied features.

In conclusion, we clearly observed an unusual evolution of PAD in a photon energy range of $h\nu$ = 7 eV ~ 8 eV which is caused by non-trivial multi-particle photoemission events at weakly bounded interfaces. Multiple scattering theory will be helpful to understand the origin of the PAD and hence to reveal the modification of the molecular orbital upon weak interactions.

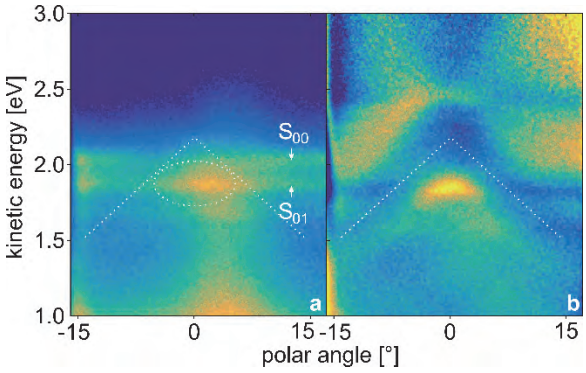

Fig. 1. (a) LE-ARUPS intensity map for PEN(0.3 nm)/HOPG taken at 15 K and normal emission using $h\nu$ = 7.4 eV; and (b) the average of 5 maps using $h\nu$ = 7.4 eV ~ 7.8 eV, normalized by its horizontally and vertically integrated profiles.

[1] S. Tanaka *et al*., Sci. Rep. **3** (2013) 3031.
[2] T. Yamaguchi *et al*., UVSOR Activity Report 2015 **43** (2016) 135.
[3] T. Yamaguchi *et al*., UVSOR Activity Report 2016 **44** (2017) 151.
[4] T. Yamaguchi *et al*., UVSOR Activity Report 2017 **45** (2018) 142.
[5] S. K. Mahatha *et al*., Phys. Rev. B **84** (2011) 113106.

BL7U

Band Structure Modification of 2D TMDCs Using a Molecular Dopant

S. Park, T. Schultz, P. Amsalem, X. Xu and N. Koch
Humboldt-Universität zu Berlin, Institut für Physik, Brook-Taylor-Str. 6, 12489 Berlin, Germany

The aim of the proposed experiments was to achieve a deep understanding of the microscopic phenomena occurring upon interface formation between a MoS_2 monolayer and a strong electron acceptor molecule, F_6TCNNQ, which can be employed for p-doping of semiconductors [1]. In the initially planned experiments, several substrates including sapphire, HOPG and silver, were to be employed as support for the MoS_2 film.

During the experiments at BL7U, we first encountered charging issues when using sapphire as support, though the very same sample could be successfully measured in-house by photoemission using a standard helium discharge lamp. Most of the remaining time was then dedicated to high resolution measurements of MoS_2/HOPG with and without F_6TCCNQ and at different temperatures ranging from 7 K to 300 K. For this system, we first observed by angle-resolved photoemission (ARPES) that the electronic band structure could be nicely resolved, as exemplified in Fig. 1, though the MoS_2 monolayer is azimuthally disordered. Such an observation is enabled by selective high photoemission intensity along Γ-K and Γ-M of the single crystal which singles out these features also after azimuthal integration. These first results are included in a manuscript that has been submitted for publication [2].

Regarding the initial aim of this project, we could successfully demonstrate that p-doping of the MoS_2 film on HOPG occurs upon F_6TCCNQ deposition. This is shown in Fig. 1 in which the MoS_2 valence band (VB) features are seen to shift to lower binding energies by up to 0.26 eV upon molecular adsorption. Interestingly, we also observed that the MoS_2 VB shifts are temperature-dependent and p-doping is found less effective at low temperatures. The measurements indicate that p-doping results from charge transfer to the F_6TCNNQ, giving rise to partial filling of the lowest unoccupied molecular orbital (LUMO). Further high-resolution measurements of the low binding energy region corresponding to the partially-filled LUMO states, revealed temperature-dependent magnitude of the charge transfer with a critical temperature of ca. 100 K as shown in Fig. 2. Deep understanding of the charge transfer mechanisms as unraveled in this experiment will lead to strong insight into the physics involved in TMDC doping by adsorption of small organic molecules with strong electron acceptor properties.

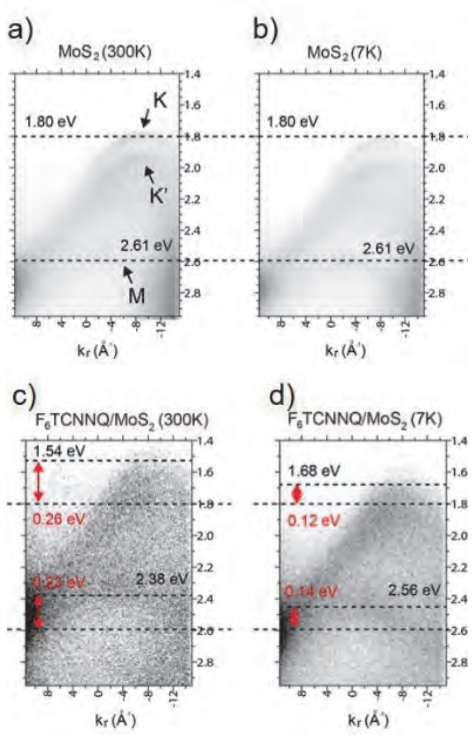

Fig. 1. a) and b) ARPES spectra of clean MoS_2/HOPG around the K point of the Brillouin zone at 300 K and 7 K, respectively. c) and d) corresponding ARPES spectra after deposition of F_6TCNNQ. (hν = 21 eV)

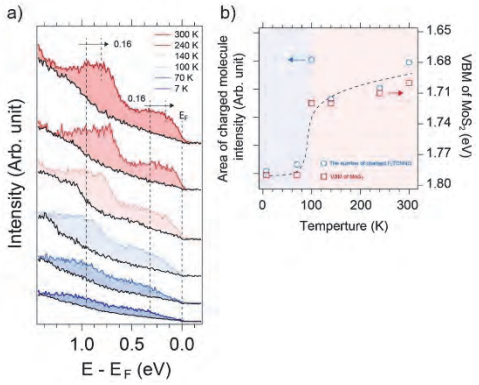

Fig. 2. a) Temperature-dependent energy distribution curve of MoS_2/HOPG near the Fermi-level, before (black) and after (colored) F6TCNNQ deposition. The additional density of states after molecular deposition is due to charged molecules only. b) Area of the signal due to charged molecules and energy shift of the MoS_2 VB as a function of temperature. The critical temperature occurs at ca. 100 K.

[1] T. Schultz *et al.*, Physical Review B **93** (2016) 125309.
[2] S. Park *et al.*, Comm. Phys. (submitted).

BL7U

UPS Measurement of Valence Electronic States in Dinaphtho[2,3-b:2', 3'-f]thieno[3,2-b]thiophene Single Crystals

R. Takeuchi[1], S. Izawa[2], R. Tsuruta[1], S. Yamanaka[1], M. Iwashita[1], K. Tonami[1], S. Ideta[2], K. Tanaka[2], M. Hiramoto[2] and Y. Nakayama[1]

[1]*Department of Pure and Applied Chemistry, Tokyo University of Scienece, Noda 278-8510, Japan*
[2]*UVSOR Synchrotron Facility, Institute for Molecular Science, Okazaki 444-8787, Japan*

Dinaphtho[2,3-b:2',3'-f]thieno[3,2-b]thiophene ($C_{22}H_{12}S_2$, DNTT, Fig. 1) attracts attention as a high-mobility p-type organic semiconductor material [1]. One of the problems of organic semiconductor materials such as pentacene is their low stability in the atmosphere. DNTT is proposed to be more robust against oxidation than pentacene [2], and has been regarded as a promising material for applications. However, the valence electronic structure that contributes to its charge transport is not fully understood, and researches using the single crystals are necessary to obtain knowledge about the fundamental electronic structure [3]. In this study, the valence electron structure of the single crystal of DNTT was measured by ultraviolet photoelectron spectroscopy (UPS).

DNTT single crystals were prepared by a physical vapor transport (PVT) technique. The crystals were attached to gold-coated silicon substrates using silver paste in order to avoid sample charging. UPS measurements were conducted at BL7U, UVSOR, using an electron spectrometer A-1 (MBS) or at an offline apparatus equipped with DA-30 (Scienta-Omicron). For the offline UPS measurements, He-IIα light source (hν = 40.81 eV) was used, and the work function value of the electron spectrometer was determined to be 4.37 eV from the Fermi edge position. In this study, a 375 nm laser was irradiated at the same time in order to avoid sample charging. All UPS measurements were conducted at room temperature.

Figure 2 shows a UPS spectrum of a DNTT single crystal sample taken at hν = 10 eV. Whereas three components were barely recognized in the binding energy (BE) range of -3.5 ~ -0.5 eV, the highest occupied molecular orbital (HOMO)-derived peak was not resolved clearly.

In contrast, UPS results taken at hν = 40.81 eV clearly exhibited the HOMO-derived peak as shown in Fig. 3 (left), which allowed the determination of the valence band maximum (VBM) of the DNTT single crystal to be -0.69 eV. Figure 3 (right) shows a photoemission spectrum in the secondary electron cutoff region from the sample being biased at −5 V, where the abscissa is rescaled to indicate the work function. The work function of the DNTT single crystal was determined to be 4.30 eV from the onset position. From these results, the ionization energy of the DNTT single crystals is determined to be 4.99 eV, which is significantly smaller than that reported previously for the DNTT thin film (5.44 eV [2]).

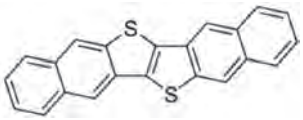

Fig. 1. Molecular structure of DNTT.

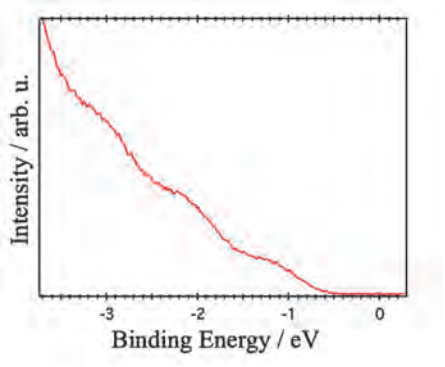

Fig. 2. UPS spectrum of the DNTT single crystal taken at BL7U (hν = 10 eV).

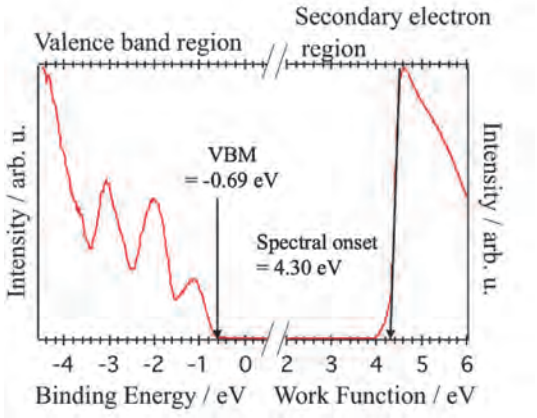

Fig. 3. UPS spectra of the DNTT single crystal in the HOMO region (left) and secondary electron cutoff region (right) taken with He-IIα excitation.

[1] T. Yamamoto and K. Takimiya, J. Am. Chem. Soc. **129** (2007) 2224.
[2] H. Yagi *et al*., Chem. Phys. Lett. **563** (2013) 56.
[3] X. Wei *et al*., Adv. Mater, **25** (2013) 3478.

BL7U

Two-Dimensional Nature of Topological Surface States on SmB_6(111) Clarified by Synchrotron-Radiation Angle-Resolved Photoelectron Spectroscopy

Y. Ohtsubo[1,2], Y. Yamashita[2], T. Nakamura[2], S. Ideta[3], K. Tanaka[3], W. Hirano[4], F. Iga[4] and S. Kimura[1,2]

[1]*Graduate School of Frontier Biosciences, Osaka University, Suita 565-0871, Japan*
[2]*Department of Physics, Graduate School of Science, Osaka University, Toyonaka 560-0043, Japan*
[3]*UVSOR Synchrotron Facility, Institute for Molecular Science, Okazaki 444-8585, Japan*
[4]*College of Science, Ibaraki University, Mito 310-8512, Japan*

Topological Kondo Insulators (TKI) are gathering much attention in these days as a promising playground to study the concert effect of the spin-polarized topological surface states and strong electron correlation resulting in the metal-insulator transition of Kondo insulators [1]. SmB_6 is the first and the most extensively studied candidate of TKI. It has been revealed that the (001) surface of the cleaved SmB_6 single crystal hosts the metallic and spin-polarized surface states as expected from topological classification [1, 2]. However, the topological order of SmB_6 itself is still under debate because of the multiple possible interpretations of the metallic surface bands [3].

We have studied the surface electronic structure of SmB_6 in these years to reveal its topological order as well as the non-conventional electronic phenomena driven by strong electron correlation [4, 5]. Before this project, we have already discovered the metallic electronic states with spin polarization on the (111) surface of SmB_6 [4, 5]. However, its dimensionality, two-dimensional (2D) surface-derived ones or three-dimensional (3D) bulk bands, had not been clear yet.

In this project, we performed angle-resolved photoelectron spectroscopy (ARPES) measurements on the SmB_6(111) surface and carefully traced the incident photon energy dependence of the metallic band S1 and the other band lying just below S1, namely S2, as shown in Fig. 1 (a), to elucidate k_z-dependent band dispersions, if it exists.

Figures 1(b) and 1(c) show the ARPES momentum distribution curves (MDCs) corresponding to S1 and S2, respectively. As evidently shown there, the S1 peak positions shown in Fig. 1(b) are independent from the incident photon energy, indicating its 2D nature, implying to originate from the surface electronic structure. As for S2 in Fig. 1(c), the behavior is similar to S1, suggesting the common 2D origin. However, one can find broad humps changing its center positions depending on the photon energies, such as that at +0.3 $Å^{-1}$ with $h\nu$ = 20 eV. Because of these photon-energy-dependent features, we cannot exclude possible 3D character for S2 from these data.

Based on the current data, we could conclude that the metallic electronic state at the Fermi level, S1, is from the surface electronic structure without any ambiguity. Together with the former results, we propose the topologically non-trivial picture of SmB_6 [4, 5].

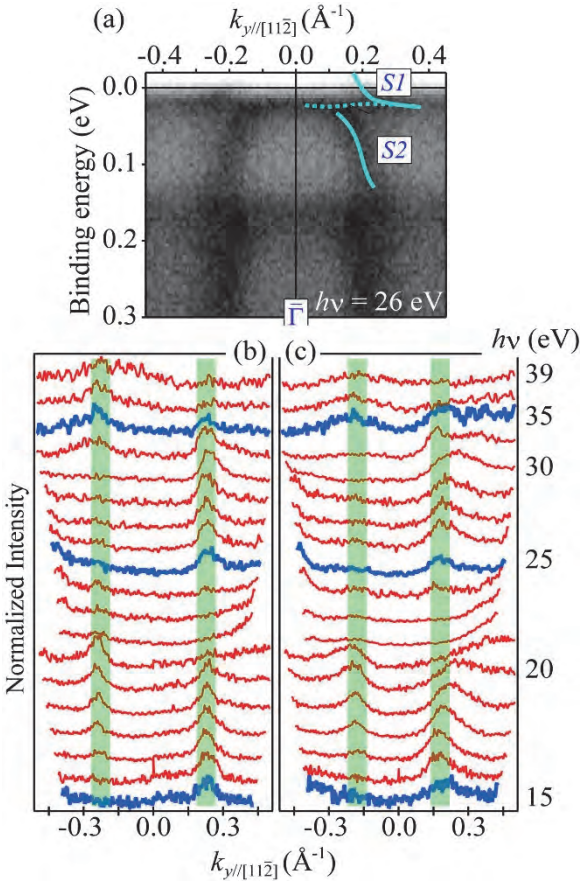

Fig. 1. (a) ARPES intensity plot of SmB_6(111) taken at hν = 26 eV and 15 K. (b, c) ARPES MDCs at 15 K with elevating photon energies. The binding energies are (b) 0 meV (Fermi level) and (c) 60 meV, corresponding to the bands S1 and S2 in (a), respectively.

[1] M. Dzero *et al.*, Phys. Rev. Lett. **104** (2010) 106408.
[2] N. Xu *et al.*, J. Phys.: Condens. Matt. **28** (2016) 363001 and references therein.
[3] P. Hlawenka *et al.*, Nat. Commun. **9** (2018) 517.
[4] Y. Ohtsubo *et al.*, arXiv: 1803.09433 (2018).
[5] Y. Ohtsubo *et al.*, UVSOR Activity Report 2016 **44** (2017) 138.

UVSOR User 6